Magnetic ordering and spin-liquid state of $YMnO_3$

Junghwan Park,[1] J.-G. Park,[2,3,*] Gun Sang Jeon,[2] Han-Yong Choi,[2] Changhee Lee,[4] W. Jo,[5] R. Bewley,[6] K. A. McEwen,[7] and T. G. Perring[6]

[1] *Department of Physics, Inha University, Incheon 402-751, Korea*

[2] *Department of Physics and Institute of Basic Science, SungKyunKwan University, Suwon 440-746, Korea*

[3] *Center for Strongly Correlated Materials Research, Seoul National University, Seoul 151- 742, Korea*

[4] *Neutron Physics Laboratory, Korea Atomic Energy Research Institute, Daejon 305-600, Korea*

[5] *Geballe Laboratory for Advanced Materials, Stanford University, California 94305, USA*

[6] *ISIS Facility, Rutherford Appleton Laboratory, Chilton, Didcot OX11 0QX, United Kingdom*

[7] *Department of Physics and Astronomy, University College London, Gower Street, London WC1E 6BT, United Kingdom*

(Received 28 June 2002; revised manuscript received 12 February 2003; published 23 September 2003)

We have measured the bulk properties as well as the elastic and inelastic neutron scattering of $YMnO_3$ in order to understand the static and dynamic properties of the Mn moments. Our measurements clearly show that above T_N there are short range correlations between spins at the nearest neighbor and next nearest neighbor Mn sites, which also fluctuate in time. This, together with other bulk properties, demonstrates the presence of a spin liquid phase above T_N arising from the geometrically frustrated Mn moments. Below T_N, a well-defined spin wave develops and we can understand the experimentally measured spin wave spectrum in terms of a Heisenberg Hamiltonian with a small easy plane anisotropy. However, even in the ordered phase we have found evidence of short range spin correlations.

DOI: 10.1103/PhysRevB.68.104426 PACS number(s): 75.25.+z, 75.40.Gb, 75.40.Cx, 75.50.Ee

I. INTRODUCTION

Physics arising from high ground state degeneracy is abundant in nature, and has attracted much interest recently. Such examples can be found in very diverse fields of research, and consequently understanding their thermodynamic properties has far reaching implications.[1] A magnetic example of such a system occurs when the competing interactions, typically of the order of the Curie-Weiss temperature θ_{CW}, cannot find a way to order at temperatures of the magnetic interaction because of the special geometrical arrangement of spins. Either they do not order at all, or if they do their ordering temperature is much lower than θ_{CW}. These so-called geometrically frustrated systems include different classes of materials. For example, $SrCr_{9p}Ga_{12-9p}O_{19}$ has a 2D network of corner-sharing triangles, the so-called *kagome* lattice,[2] and a 3D version of the corner-sharing triangular spin network is $Gd_3Ga_5O_{12}$.[3] Examples of 3D geometrically frustrated lattices include the pyrochlore compounds.[4]

Rare-earth manganese oxides, $RMnO_3$ form in two crystallographic structures depending on the ionic radius of the rare-earth elements. For rare-earth elements with a small ionic radius, Ho, Er, Tm, Yb, Lu, and Y, it has the hexagonal structure[5] while the orthorhombic perovskite structure is found in $RMnO_3$ with a large ionic radius, La, Pr, Nd, Sm, Eu, Gd, and Tb.[6] We note that some of the hexagonal manganites can also form in the orthorhombic structure depending on the heat treatment. Unlike the recently extensively studied perovskite manganites that show colossal magnetoresistance behavior, the hexagonal $RMnO_3$ compounds have a ferroelectric transition at very high temperature: e.g., $T_C \sim 900$ K for $YMnO_3$, and an antiferromagnetic transition at a much lower temperature, e.g., $T_N = 70$ K for $YMnO_3$.[7] Such compounds are known as ferroelectromagnets. Furthermore, the hexagonal manganites remain insulating over the whole temperature range.

What is particularly interesting from the viewpoint of geometrically frustrated magnetism is that the Mn ions form a natural 2D network of corner-sharing triangular network, which leads to frustration. In this paper, we have not only investigated the bulk properties of $YMnO_3$ but also measured the elastic and inelastic neutron scattering above and below the antiferromagnetic transition. What distinguishes $YMnO_3$ apart from other well-documented 2D spin systems[8] is that it is a geometrically frustrated system, which is 2D Heisenberg system having a very small easy plane anisotropy. For example, most of the ABX_3 compounds that are Heisenberg-triangular antiferromagnets with an easy plane anisotropy have strong chain interactions, i.e., they are quasi one dimensional.[8] Other examples of such 2D Heisenberg systems are anhydrous alums that are known to have weak Ising-type anisotropy.[9] Our studies also reveal that $YMnO_3$ has a spin liquid phase, which is present well above T_N. Moreover, short range spin correlations seem to exist even below T_N. In the antiferromagnetic phase, the ordered moments lie in the basal plane with a reduced value of $3.30\mu_B$ per Mn atom.

II. EXPERIMENTAL DETAILS

For our experiments, we used $YMnO_3$ of 99.9% purity from Superconductive Components, Inc. Our neutron diffraction measurements show no trace of known impurities such as Mn_3O_4, Y_2O_3, etc. We measured the magnetization using a commercial magnetometer (PPMS9, Quantum Design) from 2 to 300 K. We also used a commercial vibrating sample magnetometer (Lakeshore VSM 7300) in order to measure the magnetization from 300 to 800 K. Our neutron diffraction experiments were carried out from 10 to 300 K

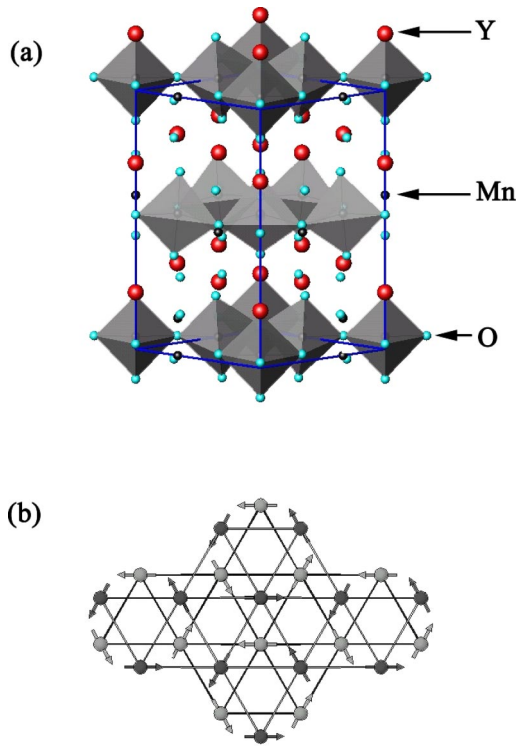

FIG. 1. (Color online) (a) Crystal structure of $YMnO_3$ with the space group of $P6_3cm$. (b) Magnetic structure of Mn moments for Γ_1 representation. Filled and open circles denote Mn moments in the $z=0$ and $z=1/2$ planes, respectively.

using a neutron wavelength of $\lambda=1.834$ Å at the high resolution powder diffractometer (HRPD) of the Korea Atomic Energy Research Institute. We analyzed the data using the Rietveld program FULLPROF and made a magnetic group theoretical analysis using the program MODY-2.

Inelastic neutron scattering measurements from 5 to 700 K were made using about 52 g of powder sample with the HET chopper spectrometer at the ISIS Facility in the UK. We used a flat plate-shaped Al sample container. Most of these measurements were made with an incident energy of 40 meV. The scattering function $S(Q,\omega)$ as a function of wave vector transfer Q and energy transfer $\hbar\omega$ is obtained from the raw time-of-flight data by normalizing to the incident flux using the integral of the incident beam monitor.[10] The instrument resolution of the setup used in this work is better than 2.2 meV at the elastic peak position and 1.3 meV at the energy transfer of 20 meV.

III. EXPERIMENTAL RESULTS AND ANALYSIS

Shown in Fig. 1(a) is the crystallographic structure of $YMnO_3$ with the $P6_3cm$ space group. One notes that the Mn atoms of $YMnO_3$ form a natural 2D network separated along the c axis by a noncoplanar layer of Y atoms. The distance between the nearest Mn atoms is 3.54 and 6.05 Å for the ab plane and c axis, respectively. The analysis of our neutron diffraction data[11] shows that below T_N the Mn moments are aligned in the basal plane, in agreement with previous publications[12,13] [see Fig. 1(b)].

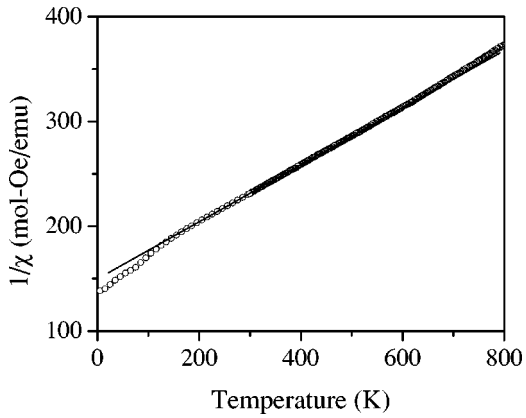

FIG. 2. Temperature dependence of the inverse susceptibility of $YMnO_3$ measured with a magnetic field of 1000 Oe.

The Mn moments are strongly coupled with $\theta_{CW}\simeq-545$ K as shown in Fig. 2. The antiferromagnetic coupling between nearest-neighbor Mn spins at the edge sharing triangular network leads to the frustration effects. In fact, $YMnO_3$ does not order until 70 K so the ratio between θ_{CW} and T_N is about 7.8.[14] From the measured Curie-Weiss temperature we estimate the nearest-neighbor exchange integral $J\approx3.8$ meV using $S=2$ for Mn^{3+} and

$$\theta_{CW}=-\frac{1}{3}qJS(S+1), \tag{1}$$

where q is the number of nearest neighbors. By interpolating the results of Capriotti *et al.*,[15,16] we then estimate the transition temperature as $T_N\approx0.3J(S+1/2)^2=85$ K for an easy-plane antiferromagnetic Heisenberg model on a triangular lattice [see Eq. (3) below] with $S=2$ and $\alpha\approx0.95$. These values are found appropriate for Mn^{3+} of $YMnO_3$. [Note that the spin wave analysis that will be discussed below Eq. (3) yields $J\approx3$ meV, which then gives $T_N\approx67$ K.] This estimate is in good agreement with the measured transition temperature $T_N=70$ K. Another noteworthy point is that the inverse susceptibility is linear from 100 to 600 K and has an upward curvature above 600 K. We can fit the data using the usual Curie-Weiss formula with a small temperature-independent background signal from the sample holder, which was measured separately. Since signals from the sample holder are less than 1% of those from the samples and do not show any drastic temperature dependence, there is a very little change even after correcting the data for the holder contributions. Moreover, the demagnetization correction is negligible over the entire temperature range as the magnetization is very small for $YMnO_3$.

Additional evidence of geometrically frustrated magnetism in $YMnO_3$ can be found in our neutron diffraction data. Apart from the usual nuclear and magnetic peaks, there is a strong diffuse scattering around $2\theta=20°$, especially in the data taken near at T_N. As one can see in Fig. 3, this diffuse scattering is almost absent in the data taken at 300 K. However, on cooling it becomes clearly observable and seems to be most pronounced around the antiferromagnetic transition temperature before it gets subdued with further cooling.

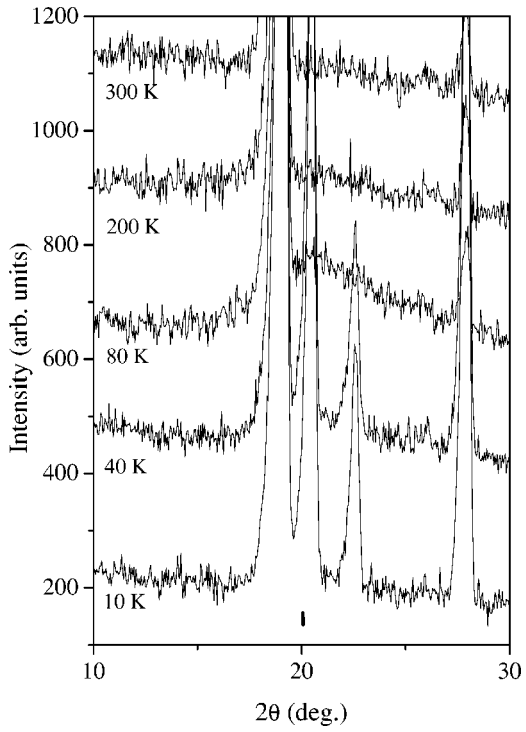

FIG. 3. We show neutron powder diffraction patterns of $YMnO_3$ for several representative temperatures from 10 to 300 K. For ease of presentation, the data are shifted upwards. The height of the bar at the bottom represents a typical size of errors.

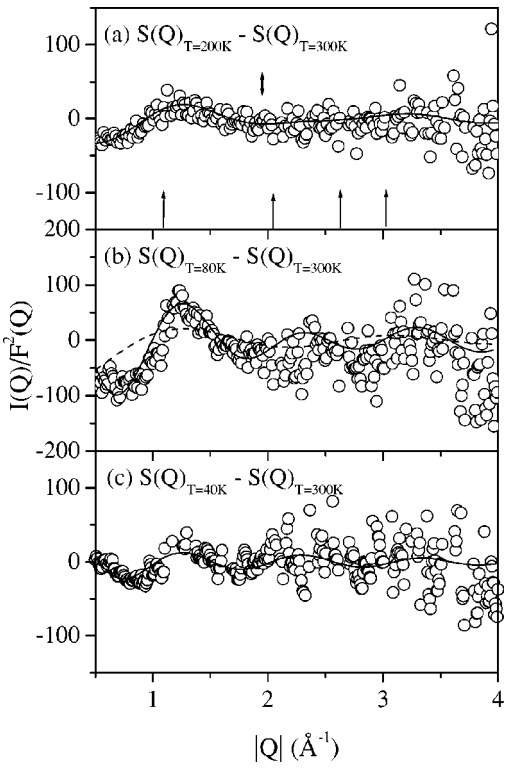

FIG. 4. Q dependence of magnetic diffuse scattering. We subtracted off the diffraction pattern taken at 300 K from the diffraction patterns taken at (a) 200, (b) 80, and (c) 40 K. We corrected the difference curve for the form factor $F(Q)$ of Mn^{3+} (see the text). Arrows at the bottom of the top panel (a) indicate the position of nuclear Bragg peaks while a double-sided arrow represents the typical size of errors. The dotted line in (b) is for spin correlations between nearest neighbors only. With an additional term for spin correlations between next nearest neighbors, the curve fitting results (full line) reproduce the experimental data well (see the text).

However, we should point out that even the data taken at 40 K, well below T_N, show a signature of the diffuse scattering [see also Fig. 4(c)]. A similarly strong diffuse scattering was previously observed in $ScMnO_3$,[13,17] another frustrated hexagonal manganite system. Therefore, it is clear that the diffuse scattering observed in both $YMnO_3$ and $ScMnO_3$ is due to geometrical frustration effects of Mn moments forming a triangular network. Our analysis using the Selyakov-Scherrer formula[18] indicates that the correlation length shows a similar temperature dependence to that of the peak intensity, and has a maximum at T_N with $\xi \sim 15$ Å.

In order to understand further the diffuse scattering, we subtracted off the diffraction pattern taken at 300 K from the data taken at 40, 80, and 200 K. Figure 4 shows the difference curve as a function of momentum transfer Q. As we are using a polycrystalline sample, our data below are given in the magnitude (Q) of the vector $\vec{Q}$. The difference curve shows a strong Q modulation with a peak at $Q \simeq 1.2$ Å^{-1}, which becomes clearer as the temperature is lowered. For the analysis of the diffuse scattering, we first assumed that the diffuse scattering arises from correlations between the nearest spins using the following formula.[19]

$$\frac{I(Q)}{F^2(Q)} \sim \sum_{i,j} \langle \vec{S}_i \cdot \vec{S}_j \rangle \frac{\sin(Qr_{ij})}{Qr_{ij}}, \qquad (2)$$

where $I(Q)$ is the measured difference curve, $F(Q)$ the form factor[20] of Mn^{3+}, and r_{ij} the distance between nearest neighboring spins: for $YMnO_3$ $r_{ij} = 3.54$ Å. This function has been successfully used to explain the diffuse scattering of other frustrated magnetic systems such as $Tb_2Ti_2O_7$.[21] The dotted line in Fig. 4(b) is for curve fitting results using Eq. (2). As one can see, it does not explain the whole difference curve particularly well. In order to resolve the disagreement between the data and the curve fitting results, we then included in our calculations additional spin correlations between the next nearest neighbors at $r_{ij} = 6.13$ Å on the basal plane. Now the agreement between the data and the curve fitting results (full line) is significantly improved. The feature around $Q \sim 2.3$ Å^{-1} is clearly due to the correlations between next nearest neighbor spins. We note that Eq. (2) for the nearest spins along the c axis separated by 6.05 Å is accidentally cancelled out under the present magnetic structure, which otherwise might explain the feature at $Q \sim 2.3$ Å^{-1}. Furthermore, the ratio between the two spin correlations in Eq. (2) is -2, which is exactly what we would expect from the magnetic structure shown in Fig. 1(b). Note that the number of nearest neighbors and next nearest neighbors on the basal plane are the same. It is also noteworthy that $2 \times r_{ij}$ with $r_{ij} = 6.13$ Å is about the same as ξ obtained above using the Selyakov-Scherrer formula. With increasing temperatures, the contribution from the correlations between next nearest neighboring spins decreases naturally, but is still

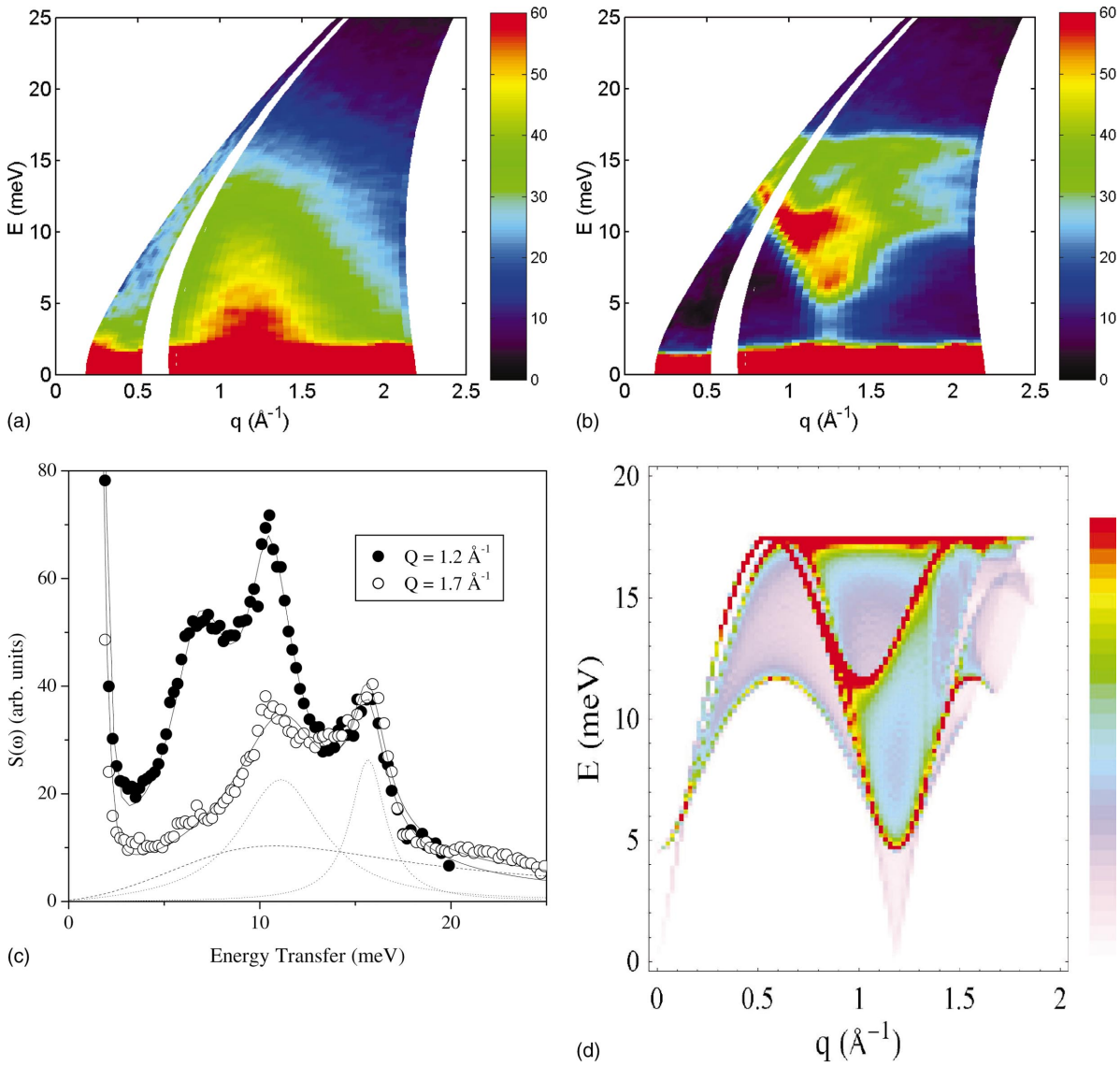

FIG. 5. (Color) Inelastic neutron scattering data taken with an incident energy of 40 meV at (a) 280 and (b) 5 K. (c) Constant Q plots of the 5 K data for $Q=1.2$ and 1.7 Å $^{-1}$. For the curve fitting of the results, we assumed two contributions to the data apart from the elastic one; one is a well-defined spin wave excitation and the other a very broad excitation. To fit the data for $Q=1.7$ Å $^{-1}$, we used two spin wave excitations (dotted lines) and a very broad excitation (dashed line). The solid lines through the two data sets for $Q=1.2$ and 1.7 Å $^{-1}$ are results of our curve fitting. (d) Theoretical calculations of the spin wave of $YMnO_3$ using the Heisenberg model with a small easy plane anisotropy (see the text).

present at 200 K as shown in Fig. 4(a). The weak presence of the correlations between next nearest neighboring spins may well be due to the fact that the temperature of 200 K is far smaller than $|\theta_{CW}|$ and even at this temperature the Mn moments are expected to be in a so-called intermediate temperature regime, i.e., still correlated. Whether the diffuse scattering exists above 200 K is not clear from the present data alone, since it becomes significantly reduced with increasing temperatures and cannot be observed within the resolution of the HRPD we used for the diffraction experiments. However, considering our other neutron scattering experiments carried out using HET we think that the diffuse scattering, albeit much smaller, indeed exists at much higher temperatures. In order to determine accurately the temperature dependence of the diffuse scattering as well as the correlation length at each temperature we need to carry out measurements on single crystal $YMnO_3$. Nevertheless, the observation of the diffuse scattering constitutes strong evidence of the spin liquid phase present in the paramagnetic phase of $YMnO_3$ arising from a geometrical frustration of Mn moments as expected from the large ratio of θ_{CW}/T_N. As shown in Fig. 4(c), this diffuse scattering is still present well below T_N. This observation clearly suggests that the ordered magnetic phase coexists with the spin-liquid state.

A further interesting feature of the short range spin correlations is revealed in the inelastic neutron scattering. Shown in Fig. 5(a) is the contour map of spin excitations measured at 280 K using polycrystalline $YMnO_3$. Even in this figure strong diffuse scattering is clearly visible near the elastic line centered at $Q\simeq 1.2$ Å $^{-1}$ in agreement with the diffraction

data discussed above. What is more interesting, however, is that this diffuse scattering appears to extend well into the inelastic region. For example, we can find a similar Q dependence of the spin excitations up to 15 meV. They all show a peak at $Q \simeq 1.2$ Å^{-1} as in the diffraction data taken at a similar temperature. This kind of feature can be found at even higher temperatures. In our measurements at higher temperatures, we can see the evidence of such spin dynamics right up to at least 500 K. Upon reducing the temperature, the magnetic excitations become stronger and, simultaneously, asymmetric around $Q \simeq 1.2$ Å^{-1}. This asymmetry in the spin excitations further develops into well-defined spin wave excitations in the antiferromagnetic phase [see Fig. 5(b)].

For the analysis of the measured spin waves in the antiferromagnetic phase, we considered two model Hamiltonians: the XY model and the Heisenberg model with an easy plane anisotropy. In our calculations following Ref. 22, it turns out that the measured spin wave spectrum of $YMnO_3$ is more compatible with the latter model. For example, the excitations around 10 meV in the experimental spin wave data cannot be described well by the XY model. Furthermore, the spin gap-like feature at $Q \simeq 1.2$ Å^{-1} can be reproduced only when we include a small easy plane anisotropy to the Heisenberg model. The easy-plane triangular antiferromagnet $YMnO_3$ was modeled in terms of the XXZ Heisenberg antiferromagetic Hamiltonian defined as follows:

$$H = J \sum_{<i,j>} [S_i^x S_j^x + S_i^y S_j^y + \alpha S_i^z S_j^z], \tag{3}$$

where i, j are the site indices on a triangular lattice, $< >$ refers to the nearest neighbors, and J is the positive exchange integral. The planar character of the system is due to the presence of the anisotropy $0 \leqslant \alpha < 1$. The minimum energy configuration of the XXZ Heisenberg antiferromagnetic Hamiltonian for $0 \leqslant \alpha < 1$ is known to be the $\sqrt{3} \times \sqrt{3}$ Néel state which consists of coplanar spins forming $\pm 2\pi/3$ angles between the nearest neighbor spins. The strength of the anisotropy near the $\sqrt{3} \times \sqrt{3}$ structure is given by $J(1-\alpha)$.[23] The interplane coupling may not be neglected, but for $YMnO_3$, whose lattice structure is shown in Fig. 1(a), the contribution of the nearest neighbor interplane coupling is expected to be much smaller for the $\sqrt{3} \times \sqrt{3}$ structure. This is because a spin in a plane is located almost at the center of three spins forming $\pm 2\pi/3$ angles between them in the nearest neighbor planes and, therefore, cancel the magnetic coupling to the nearest neighbor plane. We, therefore, neglected the interplane coupling in the present study.

Our calculations using Eq. (3) of the spin wave dispersion with $J = 3$ meV and $\alpha = 0.95$ are displayed in Fig. 5(d) after being powder averaged. We found that in our calculations there are three different spin wave branches although we could not distinguish them clearly in our experimental data because of the polycrystalline nature of our $YMnO_3$ sample. Including the anisotropy in our calculations leads to drastic effects in one lower energy spin wave branch. We note that the J value obtained from our spin wave calculation is consistent with T_N if we use a relation between the two values from theoretical calculations for the quantum easy-plane antiferromagnet on the triangular lattice.[16]

What is noticeable in both the elastic and inelastic neutron scattering data is that there is very diffusive scattering even in the antiferromagnetically ordered phase. This can be seen, for example, in the diffraction data taken at 40 K shown in Fig. 3 and the difference curve for the same data in Fig. 4(c) and the data near the elastic peak in Fig. 5(b) taken at 5 K. In order to illustrate further this point, we show constant Q plots of Fig. 5(b) for $Q = 1.2$ and 1.7 Å^{-1} [see Fig. 5(c)]. The well-defined peaks are due to spin wave excitations whereas the very broad and featureless signal is from the supposedly spin liquid phase present even in the ordered phase. This then indicates that spin fluctuations are still present and strong at temperatures as low as 5 K. Such diffuse scattering can be due either to geometrical frustration of the Mn moments at the edge-sharing triangular network, or to 2D quantum effects. Since the diffuse scattering seen at low temperatures seems to evolve continously from similar diffuse scattering above T_N, we deduce that it is more likely to be due to geometrical frustration effects. The strong spin fluctuations may well be responsible for significant entropy consumption well below the transition temperature.[24] That the ordered moment of $3.30\mu_B$ per Mn atom estimated at 10 K is much smaller than the theoretical value ($4.0\mu_B$ per Mn atom) of Mn^{3+} may well be another evidence of the presence of strong spin fluctuations in the ordered phase. On the other hand, the large θ_{CW}/T_N value for $YMnO_3$ can be partly due to the low dimensionality of the Mn networks in addition to the geometrical frustration effects.

To summarize, we have carried out bulk measurements as well as elastic and inelastic neutron scattering experiments of $YMnO_3$. From our results, we have shown clearly that above T_N there is very diffusive magnetic scattering in both space and time, indicating short range dynamic correlations which are a signature of a spin liquid phase. This spin liquid phase forms out of geometrically frustrated Mn moments. Even when they become ordered below T_N, surprisingly enough there are short range spatial correlations. Our analysis of the spin wave spectrum in the ordered phase shows that the spin waves can be well described in terms of a Heisenberg Hamiltonian with a small easy plane anisotropy. Therefore, to our knowledge $YMnO_3$ is the first such system which shows experimental evidence for both spin liquid and spin ordered phases in one sample with Heisenberg Hamiltonian with a small easy plane anisotropy.

ACKNOWLEDGMENTS

We acknowledge Seongsu Lee, H.-C. Ri, and Y. N. Choi for their help with magnetization and neutron diffraction experiments and A. N. Pirogov and S.-W. Cheong for helpful discussions. Work at SungKyunKwan University was supported by the Korea-UK collaborative research and Nuclear R & D programs of the Ministry of Science and Technology, the Center for Strongly Correlated Materials Research and Korea Research Foundation Grant No. 2000-015-DP0111. HYC and GSJ acknowledge the support from the Korea Science & Engineering Foundation through Grant No. R01-1999-00031-0 and through the Center for Nanotubes and Nanostructured Composites.

*Author to whom correspondence should be addressed. Email address: jgpark@skku.ac.kr

[1] A. P. Ramirez, *Handbook of Magnetic Materials*, edited by K. H. J. Buschow (Elsevier Science, Amsterdam, 2001), Vol. 13.

[2] A. P. Ramirez, G. P. Espinosa, and A. S. Cooper, Phys. Rev. B **45**, 2505 (1992).

[3] P. Schiffer, A. P. Ramirez, D. A. Huse, P. L. Gammel, U. Yaron, D. J. Bishop, and A. J. Valentino, Phys. Rev. Lett. **74**, 2379 (1995).

[4] For a review, see M. J. Harris and M. P. Zinkin, Mod. Phys. Lett. B **10**, 417 (1996), and references therein.

[5] H. L. Yakel, W. C. Koehler, E. F. Bertaut, and E. F. Forrat, J. Appl. Crystallogr. **16**, 957 (1963).

[6] M. A. Gilleo, J. Appl. Crystallogr. **10**, 161 (1957).

[7] G. Smolenskii and I. Chupis, Sov. Phys. Usp. **25**, 475 (1982); T. Katsufuji, S. Mori, M. Masaki, Y. Moritomo, N. Yamamoto, and H. Takagi, Phys. Rev. B **64**, 104419 (2001).

[8] For a review, see M. F. Collins and O. A. Petrenko, Can. J. Phys. **75**, 605 (1997).

[9] S. T. Bramwell, S. G. Carling, C. J. Harding, K. D. M. Harris, B. M. Kariuki, L. Nixon, and I. P. Parkin, J. Phys.: Condens. Matter **8**, L123 (1996); T. Inami, Y. Ajiro, and T. Goto, J. Phys. Soc. Jpn. **65**, 2374 (1996).

[10] J.-G. Park, K. A. McEwen, and M. J. Bull, Phys. Rev. B **66**, 094502 (2002); M. J. Bull, K. A. McEwen, and R. S. Eccleston, *ibid.* **57**, 3850 (1998).

[11] Junghwan Park, Unggul Kong, A. Pirogov, S. I. Choi, J.-G. Park, Y. N. Choi, Changhee Lee, and W. Jo, Appl. Phys. A: Mater. Sci. Process. **74**, S7961 (2002).

[12] E. F. Bertaut and M. Mercier, Phys. Lett. **5**, 27 (1963); E. F. Bertaut, M. Mercier, and R. Pauthenet, J. Phys. (France) **25**, 550 (1964).

[13] A. Munoz, J. A. Alonso, M. J. Martinez-Lope, M. T. Casais, J. L. Martinez, and M. T. Fernandez-Diaz, Phys. Rev. B **62**, 9498 (2000).

[14] This ratio of 7.8 may become smaller if we deduce θ_{CW} from higher temperature susceptibility data than given here. All our data presented in the paper indicate that the Mn moments of $YMnO_3$ are still correlated even at 200 K, i.e., in a so-called intermediate temperature range.

[15] L. Capriotti, R. Vaia, A. Cuccoli, and V. Tognetti, Phys. Rev. B **58**, 273 (1998).

[16] L. Capriotti, A. Cuccoli, V. Tognetti, P. Verrucchi, and R. Vaia, Phys. Rev. B **60**, 7299 (1999).

[17] M. Bieringer and J. E. Greedan, J. Solid State Chem. **143**, 132 (1999).

[18] L. I. Mirkin, *Handbook of X-ray Structure Analysis of Polycrystal* (Physics-Mathematics Literature, Moscow, 1961).

[19] E. F. Bertaut and P. Burlet, Solid State Commun. **5**, 279 (1967).

[20] *International Tables for Crystallography*, edited by A. J. C. Wilson (Kluwer Academic Publishers, London, 1992), Vol. C.

[21] J. S. Gardner, S. R. Dunsiger, B. D. Gaulin, M. J. P. Gingras, J. E. Greedan, R. F. Kiefl, M. D. Lumsden, W. A. MacFarlane, N. P. Raju, J. E. Sonier, I. Swainson, and Z. Tun, Phys. Rev. Lett. **82**, 1012 (1999).

[22] Th. Jolicoeur and J. C. Le Guillou, Phys. Rev. B **40**, 2727 (1989).

[23] This planar $\sqrt{3}\times\sqrt{3}$ Néel state can also be realized by introducing the onsite anisotropy to the isotropic Heisenberg Hamiltonian as $H=J\Sigma_{<i,j>}\vec{S}_i\cdot\vec{S}_j+D\Sigma_j S_j^z S_j^z$ with $D=J(1-\alpha)$.

[24] D. G. Tomuta, S. Ramakrishnan, G. J. Nieuwenhuys, and J. A. Mydosh, J. Phys.: Condens. Matter **13**, 4543 (2001).